

Secondary growth of hierarchical nanostructures composed only of Nb₃O₇F single-crystalline nanorods as a new photocatalyst for hydrogen production

Junyuan Duan,^{*ab} Guangying Mou,^a Shuai Zhang,^b Sheng Wang^b and Jianguo Guan^{*a}

^aState Key Laboratory of Advanced Technology for Materials Synthesis and Processing, Wuhan University of Technology, 122 Luoshi Road, Wuhan 430070, China. Fax: 86 27 87218832; Tel: 86 27 87218832; E-mail: guanjk@whut.edu.cn

^bQinghai Provincial Key Laboratory of New Light Alloys, School of Mechanical Engineering, Qinghai University, 251 Ningda Road, Xining 810016, China. Fax: 86 971 5310440; Tel: 86 971 5168415; E-mail: junyuanduan@sina.com

Supplementary table and images

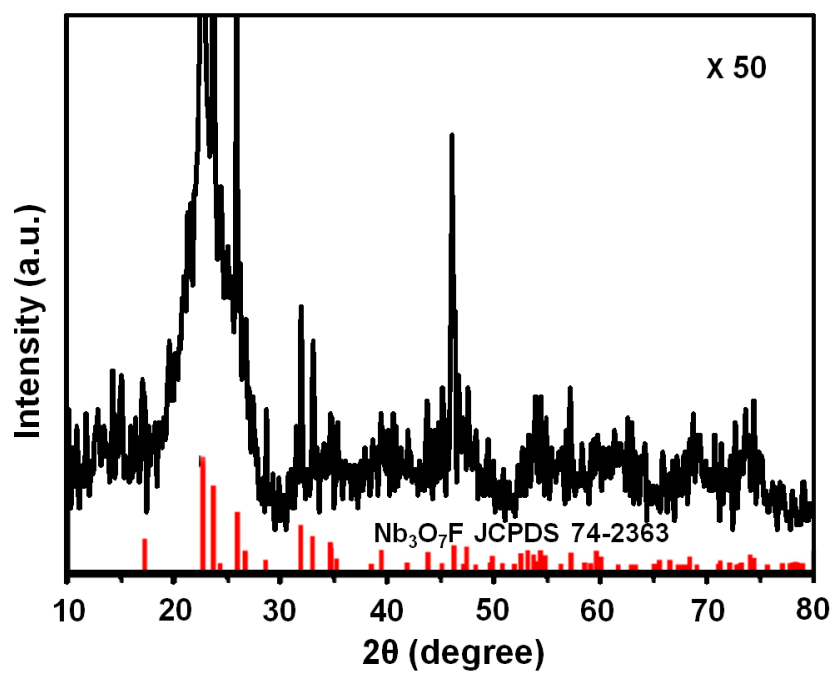


Fig. S1 The enlarged XRD pattern of Fig. 1.

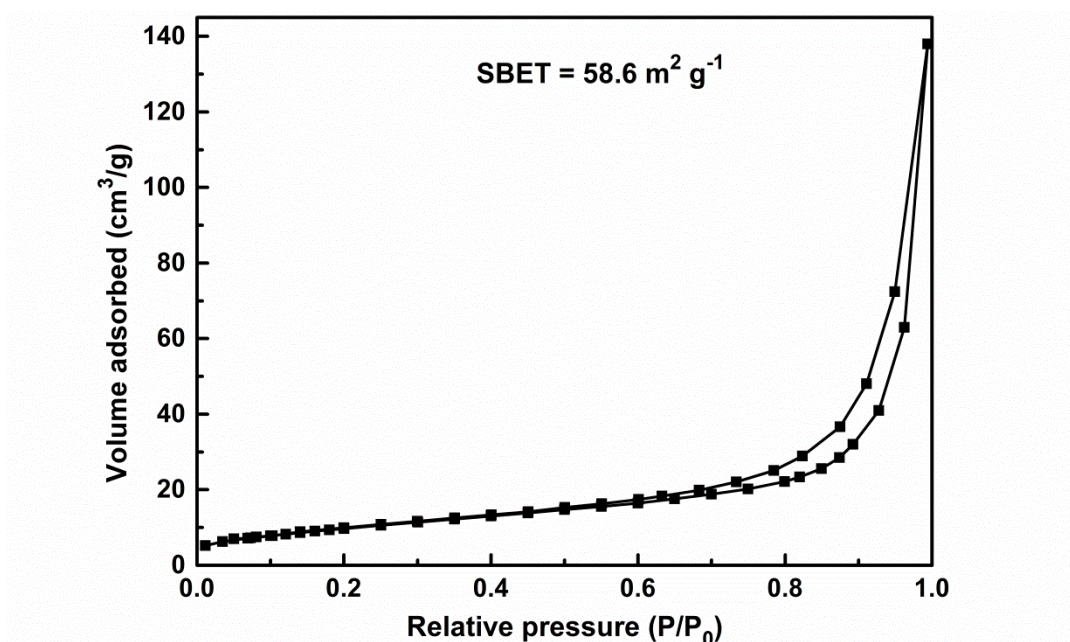


Fig. S2 Nitrogen adsorption–desorption isotherm of Nb₃O₇F HNs. Fig. S2 shows that the type H3 hysteresis loop, which is assigned to the assembly of Nb₃O₇F single crystalline nanorods giving rise to slit-like pores.^{S1} The shape of the hysteresis loop is the same as the Nb₃O₇F HNs reported in the literatures. The reported Nb₃O₇F HNs in the literatures were jointly consisted a large core in the central and nanorod in the external (Table S1). In contrast, our Nb₃O₇F HNs seems to be only consisted of nanorod units, and their nanorod units exhibit smaller diameters, giving the high specific surface area.

Table S1 Comparisons of the building units and S_{BET} of various $\text{Nb}_3\text{O}_7\text{F}$ samples

Samples	Building units	S_{BET} ($\text{m}^2 \text{g}^{-1}$)
$\text{Nb}_3\text{O}_7\text{F}$ HNs	Only Nanrods	58.6
Reference 60	Solid core in central and nanorods in external	13.15
Reference 61	Solid core in central and nanoplates in external	35.7
Reference 62	Solid core in central and nanorods in external	/

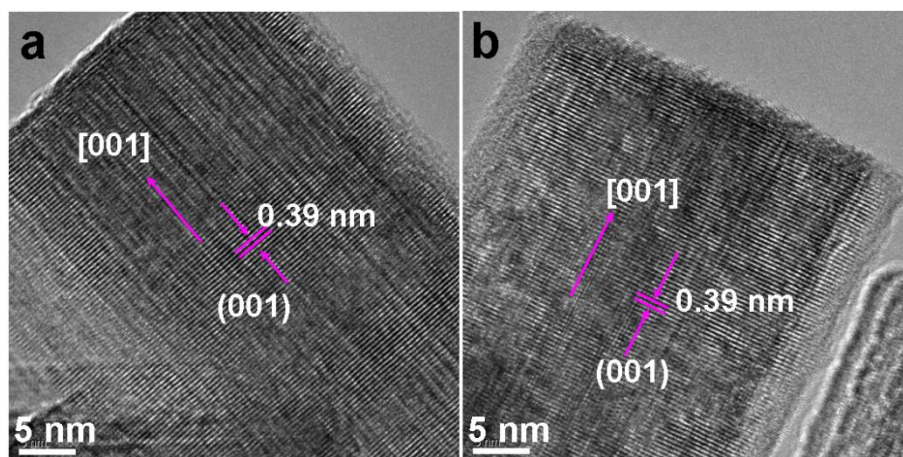


Fig. S3 HRTEM images of two individual Nb₃O₇F nanorods.

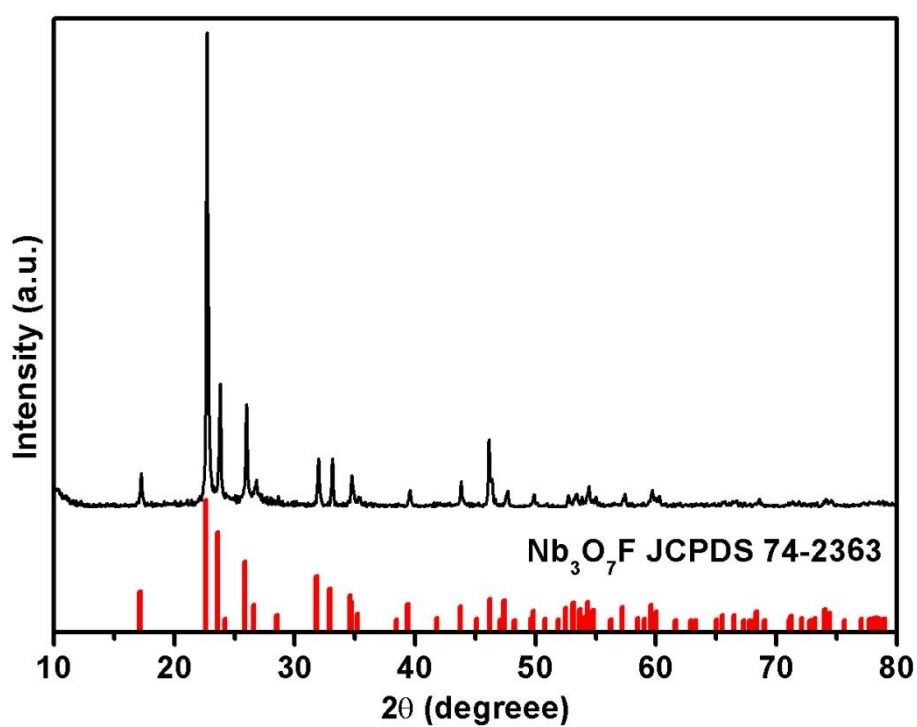


Fig. S4 XRD pattern of the Nb₃O₇F NPs-HNs obtained at $R = 30 \text{ mL}/27.5 \text{ mL}$.

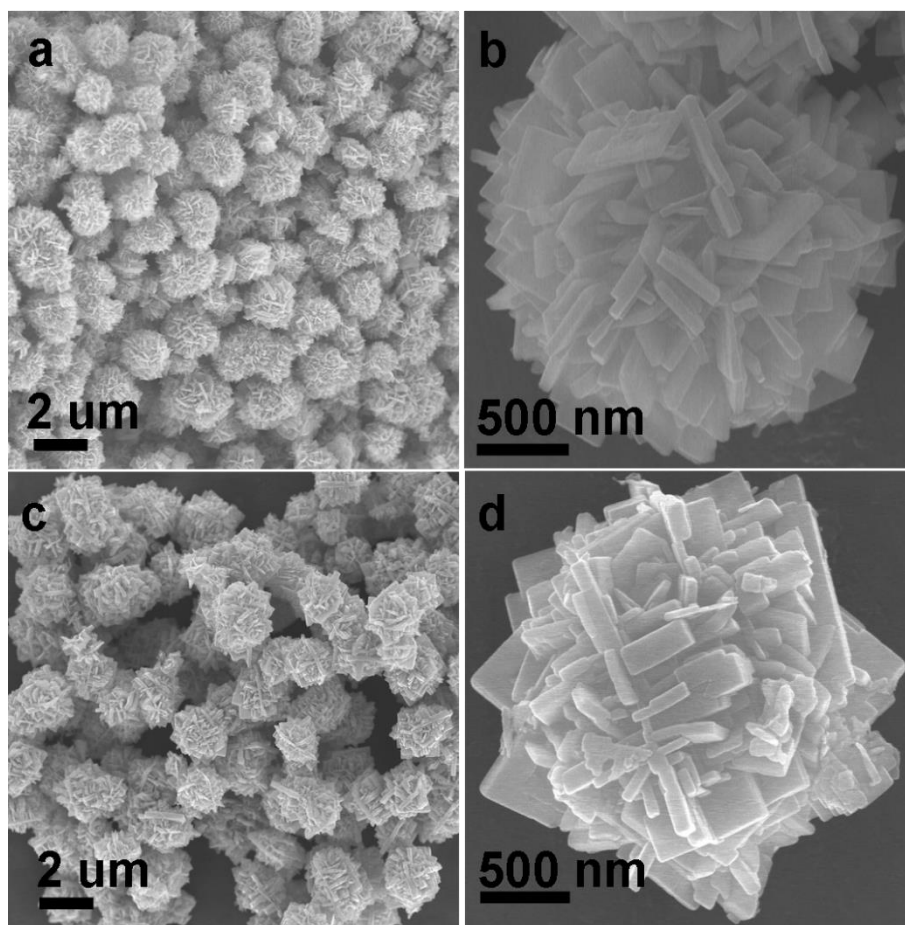


Fig. S5 SEM images of the products obtained by changing T for the synthesis of $\text{Nb}_3\text{O}_7\text{F}$ NPs-HNs to (a, b) 200 °C and (c, d) 250 °C.

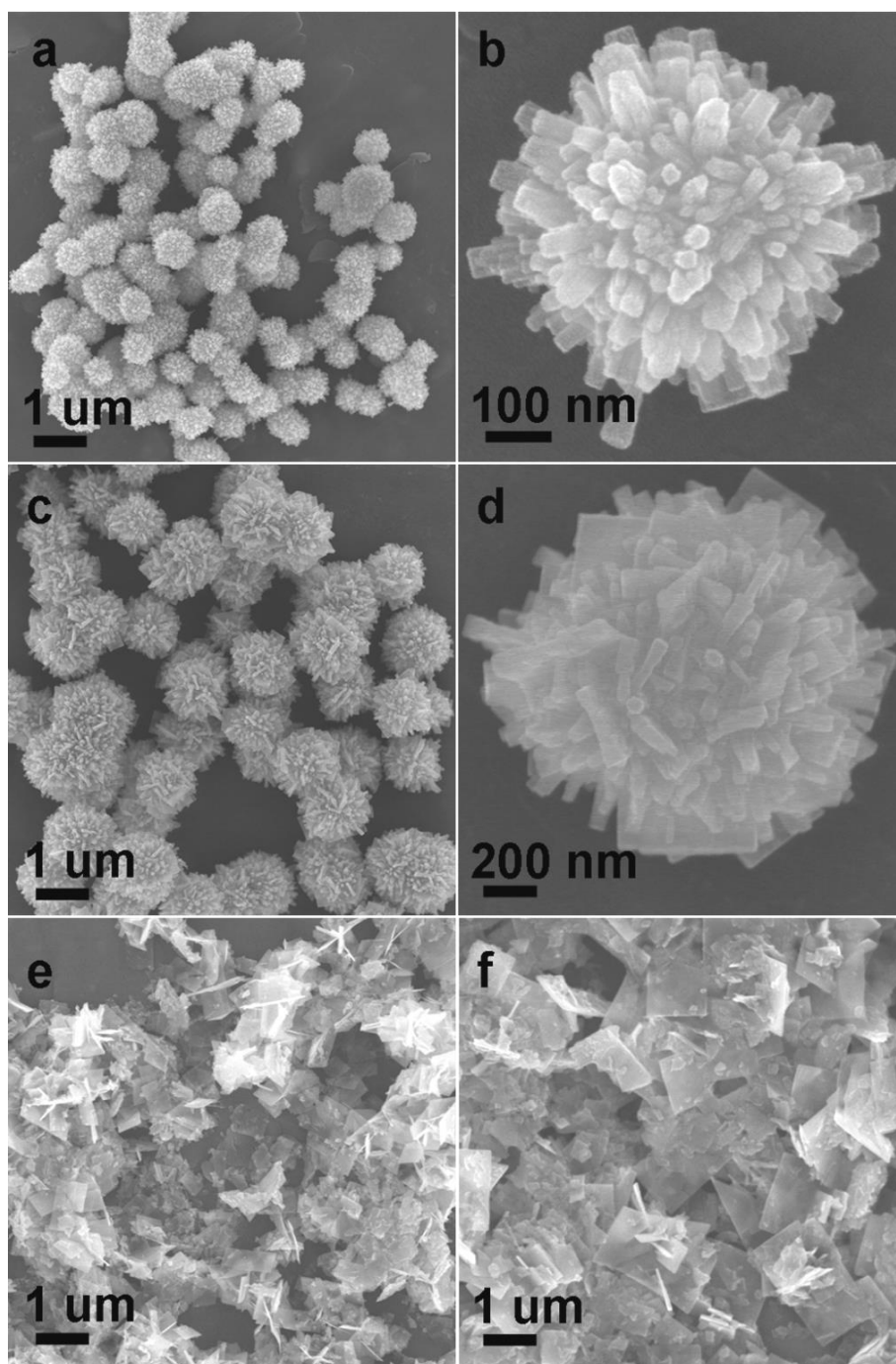


Fig. S6 SEM images of the products obtained by changing [H₂NbF₇] for the synthesis of Nb₃O₇F NPs-HNs to (a, b) 1.30 mM, (c, d) 2.60 mM, (e) 7.80 mM and (f) 10.40 mM.

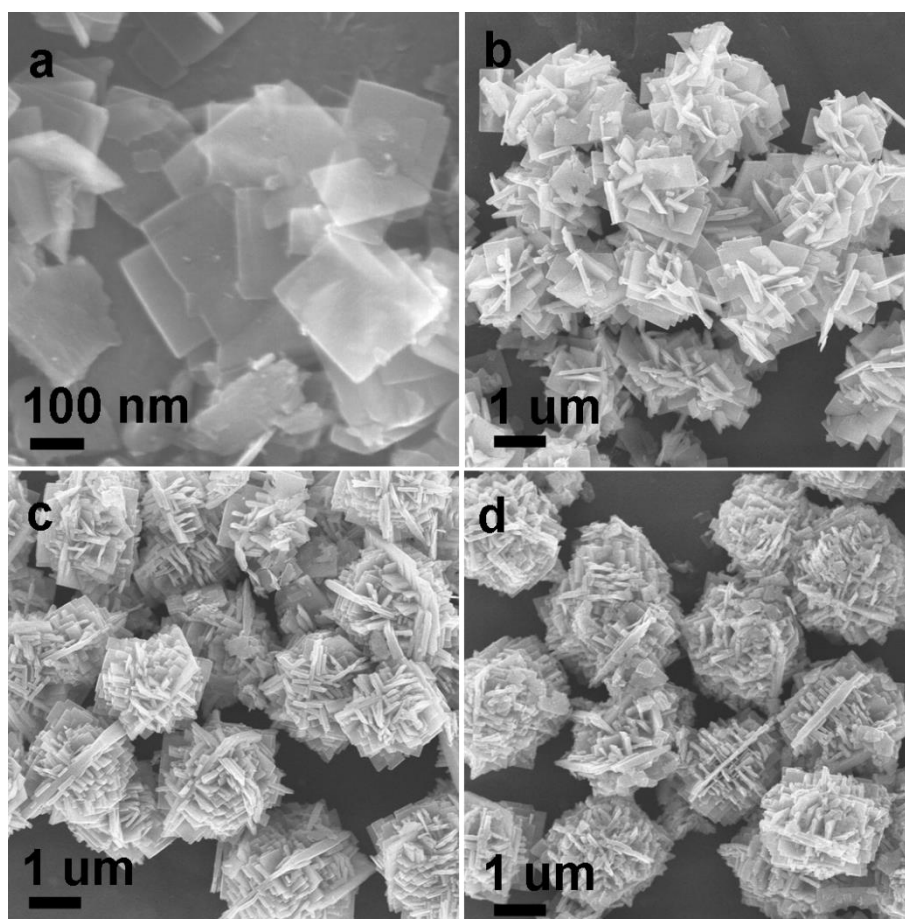


Fig. S7 SEM images of the products obtained by changing t to (a) 1 h, (b) 2 h, (c) 6 h, (d) 12 h in the synthesis of $\text{Nb}_3\text{O}_7\text{F}$ NPs-HNs.

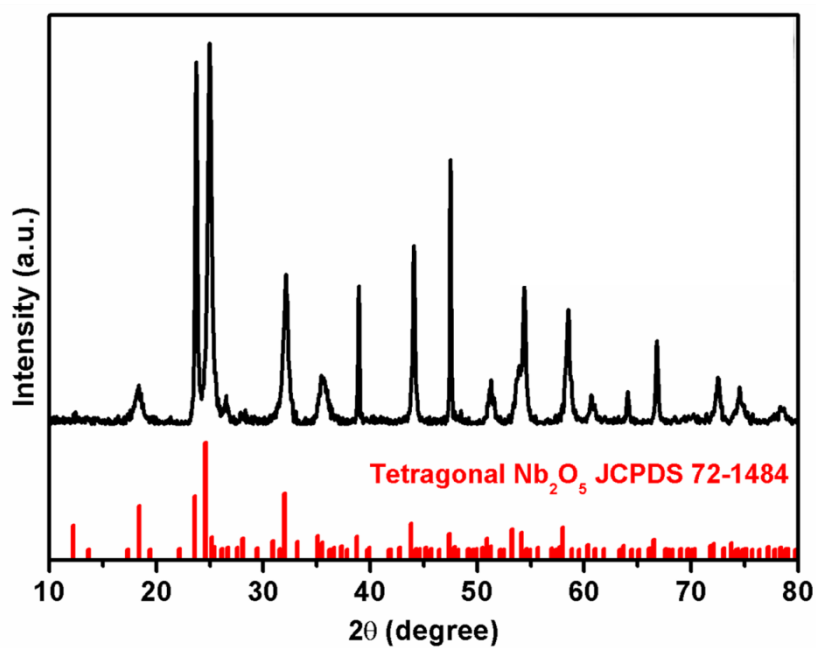


Fig. S8 XRD pattern of the products obtained by calcining $\text{Nb}_3\text{O}_7\text{F}$ HNPs at 800 °C in air atmosphere.

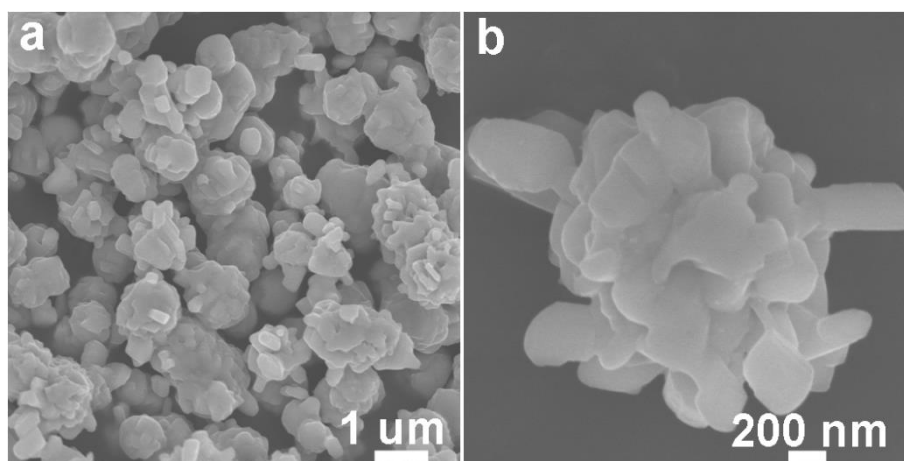


Fig. S9 SEM images of the Nb_2O_5 SPs obtained by calcining the typical $\text{Nb}_3\text{O}_7\text{F}$ HNs.

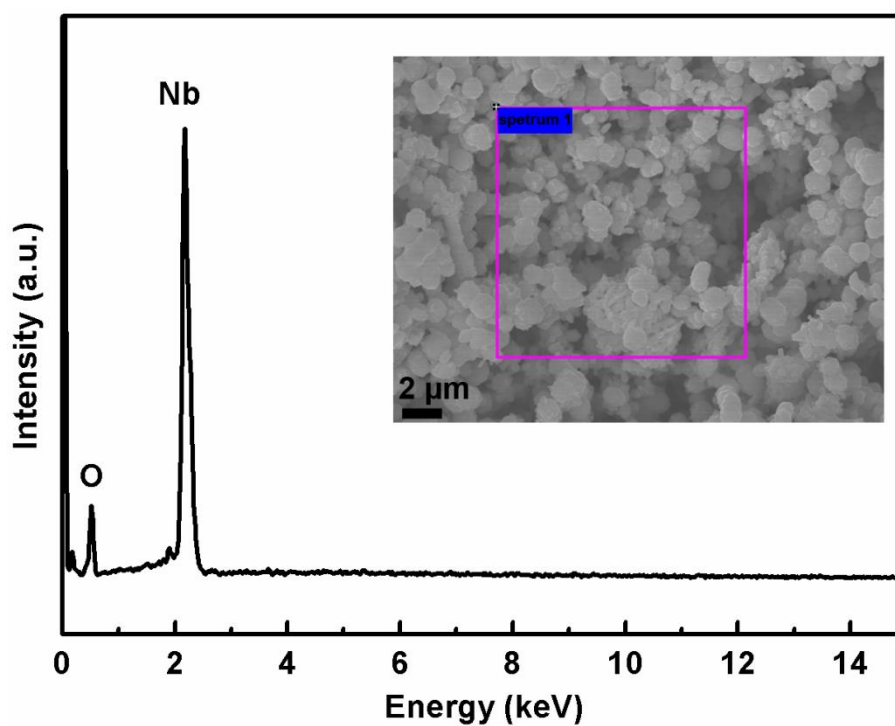


Fig. S10 EDX spectrum of the Nb_2O_5 SPs obtained by calcining the typical $\text{Nb}_3\text{O}_7\text{F}$ HNs.

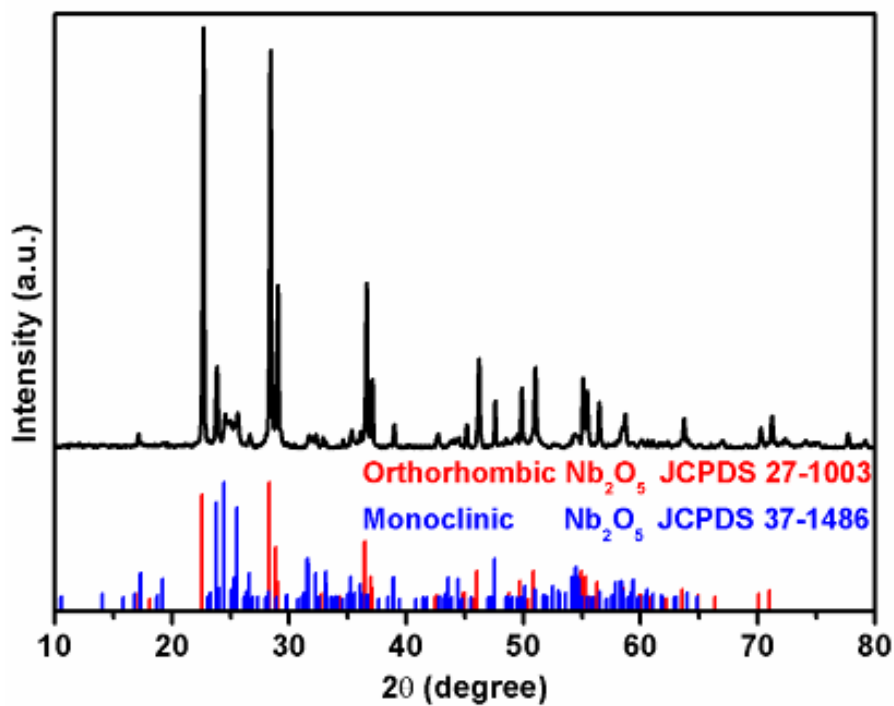


Fig. S11 XRD pattern of C-Nb₂O₅ samples.

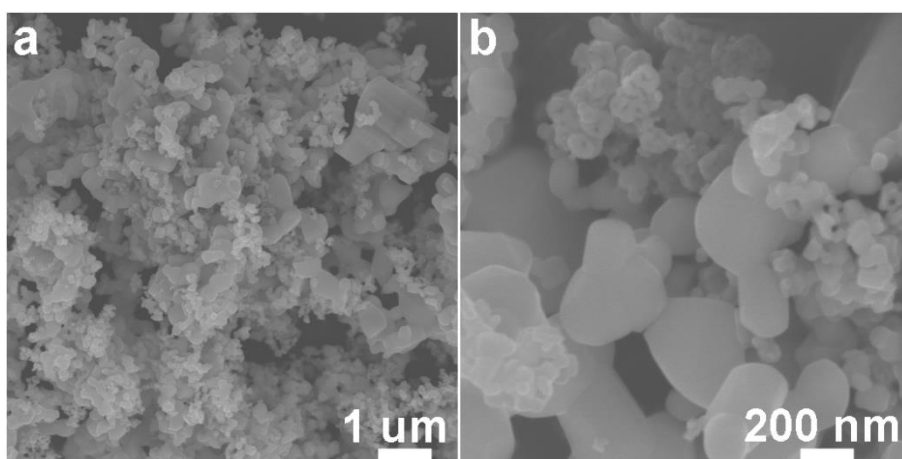


Fig. S12 XRD pattern of C-Nb₂O₅ samples.

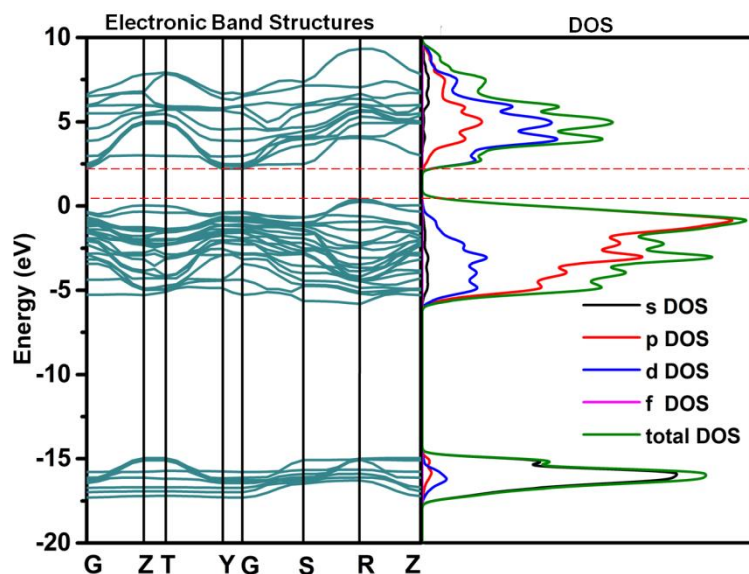


Fig. S13 Calculated (left) electronic band structures and (right) densities of states (DOS) for the unit cell of Nb₃O₇F crystals.

Calculation details

The electronic structures were calculated by using the density-functional theory-based CASTEP software package. The Perdew-Wang gradient-corrected functional for interactions between the valence electrons and ionic core and the generalized gradient approximation (GGA) were selected, and the energy cutoff was set to 340 eV.^{S2} The ultrasoft pseudopotential and $2 \times 2 \times 2$ k-point as a unit were used to calculate.^{S3} The calculated unit cell parameters of orthorhombic Nb₃O₇F: $a = 20.67 \text{ \AA}$, $b = 3.83 \text{ \AA}$ and $c = 3.93$. The geometry optimization was carried out by using the total energy with a tolerance of 2×10^{-5} eV, the forces of 0.05 eV \AA^{-1} , and the maximum atomic displacement of $2 \times 10^{-3} \text{ \AA}$.

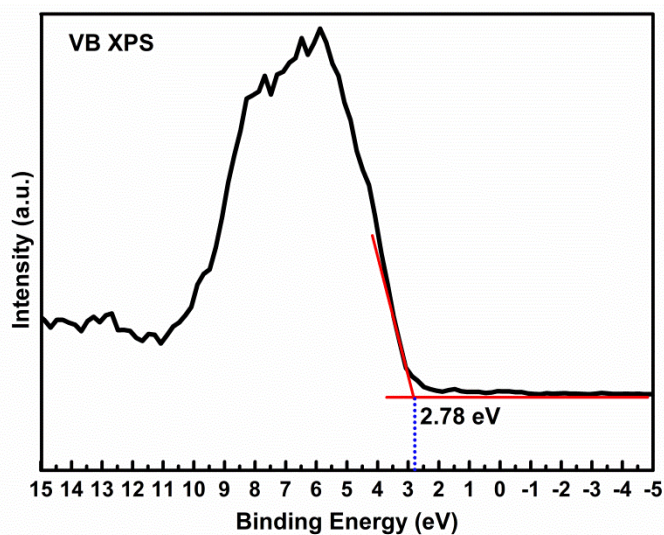


Fig. S14 XPS valence band spectrum of the $\text{Nb}_3\text{O}_7\text{F}$ HNs. The VBM was determined according to the method reported in references S4-5.

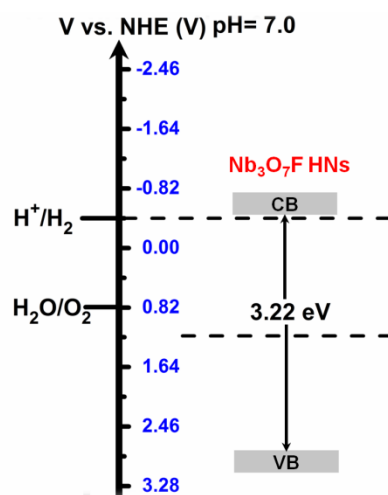


Fig. S15 Band structure diagram for the $\text{Nb}_3\text{O}_7\text{F}$ HNs dispersed in aqueous solutions at pH=7.0.

Table S2 The BET surface areas (S_{BET}) of various samples

Samples	S_{BET} (m ² /g)
Nb ₃ O ₇ F HNs	58.6
Nb ₂ O ₅ SPs	2.9
C-Nb ₂ O ₅	4.7
Nb ₃ O ₇ F NPs-HNs	31.6

References

- S1 K. S. W. Sing, D. H. Everett, R. A. W. Haul, L. Moscou, R. A. Pierotti, J. Rouquerol and T. Siemieniowska, *Pure Appl. Chem.*, 1985, 57, 603.
- S2 J. P. Perdew, J. A. Chevary, S. H. Vosko, K. A. Jackson, M. R. Pederson, D. J. Singh and C. Fiolhais, *Phys. Rev. B: Condens. Matter*, 1992, 46, 6671.
- S3 H. J. Monkhorst and J. D. Pack, *Phys. Rev. B*, 1976, 13, 5188.
- S4 G. Liu, P. Niu, L. C. Yin and H. M. Cheng, *J. Am. Chem. Soc.* 2012, 134, 9070–9073.
- S5 X. B. Chen, L. Liu, P. Y. Yu and S.S.Mao. *Science*, 2011, 331,746-750.